DMD Fast Forward. Published on March 10, 2008 as doi:10.1124/dmd.108.020669

Title page

Hepatic uptake and excretion of YM758, a novel If channel inhibitor, in rats and humans

Ken-ichi Umehara, Megumi Iwai, Yasuhisa Adachi, Takafumi Iwatsubo, Takashi Usui, and Hidetaka Kamimura

Drug Metabolism Research Laboratories, Drug Discovery Research, Astellas Pharma Inc., 1-8, Azusawa 1-chome, Itabashi-ku, Tokyo 174-8511, Japan (K.U., M.I., T.I., T.U., H.K.); ADME/TOX Research Institute, Daiichi Pure Chemicals Co., Ltd., 2117 Muramatsu, Tokai-mura, Naka-gun, Ibaraki 319-1182, Japan (Y.A.)

Running title page

Running title: Hepatic uptake and excretion of YM758 in rats and humans

Corresponding author:

Name: Ken-ichi Umehara

Address: Drug Metabolism Research Laboratories, Drug Discovery Research, Astellas Pharma Inc., 1-8, Azusawa 1-chome, Itabashi-ku, Tokyo 174-8511, Japan

Telephone: (+81) 3-5916-2155

Fax: (+81) 3-3960-6220

E-mail: kenichi.umehara@jp.astellas.com

Number of text pages: 43

Number of tables: 1

Number of figures: 10

Number of references: 40

Number of words in the Abstract: 240

Number of words in the Introduction: 675

Number of words in the Discussion: 1,337

List of non-standard abbreviations:

BCRP/Bcrp: breast cancer resistance protein

DMEM: Dulbecco's modified eagle medium

$E_2$17βG: 17β-estradiol-$_D$-17β-glucuronide

HBSS: Hank's balanced salt solution

hOCT/rOct: human organic cation transporter /rat organic cation transporter

If channel: 'funny' If current channel

MDR1/Mdr1: multidrug resistance 1

MPP: 1-methyl-4-phenylpyridinium

MRP2/Mrp2: multidrug resistance associated protein 2

rOatp2: rat organic anion transporting polypeptide 2

OATP1B1/OATP-C/OATP2: organic anion transporting polypeptide 1B1/-C/2

OATP1B3/OATP8: organic anion transporting polypeptide 1B3/8

ORF: open reading frame

PBS: Dulbecco's modified phosphate-buffered saline

DMD Fast Forward. Published on March 10, 2008 as DOI: 10.1124/dmd.108.020669
This article has not been copyedited and formatted. The final version may differ from this version.

ABSTRACT

YM758, a novel If channel inhibitor, is being developed as a treatment for stable angina and atrial fibrillation. The hepatic uptake/excretion of YM758 was clarified using transporter-expressing mammalian cells and hepatocytes mainly in humans and partly in rats. cDNA-expressing HEK293 cells were used to determine that YM758 was greatly taken up via OATP1B1 and slightly via hOCT1/rOct1, but not via OATP1B3. In addition, the uptake of $E_2$17βG via OATP1B1 was inhibited in the presence of YM758, whereas that via OATP1B3 was not. In contrast, time-dependent uptake of YM758 into rat/human hepatocytes at 37 °C was observed, as was concentration-dependent uptake into human hepatocytes (K_m value of 87.9 μmol/l). This saturable uptake of YM758 into human hepatocytes was inhibited in the presence of quinidine (an inhibitor for OATP1B1), but not cimetidine (an inhibitor for hOCT family). Moreover, the permeation clearance ratios for the transcellular transport of YM758 across MDR1-expressing LLC-PK1 cells were extensively higher than those across LLC-PK1 cells, which indicates that MDR1-mediated transport is one of the possible pathways through which YM758 may be excreted into the bile. These results indicate that YM758 is taken up into hepatocytes mainly via OATP1B1, but not via hOCT1, and is excreted into the bile via MDR1 in humans; however,

passive diffusion or an unknown uptake/excretion mechanism could be at work in the hepatocytes. This study is the first to clarify the saturable hepatic uptake and/or the excretion mechanism by the If channel inhibitor.

Myocardial ischemia always results from a disparity between oxygen supply and demand, and this debt may lead to irreversible myocardial damage. As heart rate is a major determinant of myocardial oxygen consumption (Laurent et al., 1956, Sonneblick et al., 1968), agents such as β-adrenoreceptor antagonists or some calcium channel blockers that can reduce sinus heart rate are of great interest for the treatment of ischemic heart disease (Buckberg et al.,1972), although these agents may cause concominant negative inotropic and hypotensive effects (Opie et al.,1989). Recently, the pharmacological properties of a novel class of specific bradycardic agents such as zatebradine and ivabradine have been clarified, and these compounds have reportedly reduced heart rate in clinical trials without any concomitant negative inotropic or hypotensive effects; in fact, ivabradine recently entered the market as an agent for stable angina (Indolfi et al., 1989, Roth et al., 1993, Bucchi et al., 2007). It was also reported that the heart rate reduction induced by this kind of agent was due to the inhibition of the If channel (‘funny’ If current channel) expressed in the sinus node (Bucchi et al., 2007). YM758 monophosphate, (-)-N-{2-[(R)-3-(6,7-dimethoxy-1,2,3,4-tetrahydroisoquinoline-2-carbonyl)piperidino]ethyl}-4-fluorobenzamide monophosphate is also a novel If channel inhibitor that was under development for stable angina and atrial fibrillation by Astellas Pharma Inc. (Fig. 1).

Drug disposition in hepatocytes starts with penetration through the sinusoidal membrane, followed by intracellular metabolism and/or biliary excretion (Muller et al. 1997, Yamazaki et al. 1996). Therefore, the hepatic uptake process is an important determinant of the hepatic clearance of drugs. The human/rat organic cation transporters (hOCT1/rOct1) have been identified as the specific transporters for the uptake of small hydrophilic organic cations (Koepsell et al. 2003). In humans, hOCT1 (also known as SLC22A1) is expressed predominantly on the sinusoidal membrane of hepatocytes, but in rats, Oct1 expression is highest in the kidney, with detectable expression in the liver and intestine (Koepsell et al. 2003). In addition, organic anion transporting polypeptide (OATP) 1B1 (previously OATP-C/OATP2) and OATP1B3 (previously OATP8) among several OATPs are expressed mainly on the sinusoidal membrane of hepatocytes. They are also thought to be involved in the transport of a wide variety of bulky compounds, including clinical drugs such as 3-hydroxy-3-methylglutaryl CoA reductase inhibitors (statins), from the blood into hepatocytes in humans (Ishiguro et al., 2006). The substrate specificity of OATP1B3 commonly overlaps that of OATP1B1, so several compounds, such as 17β-estradiol-$_D$-17β-glucuronide ($E_2$17βG), pitavastatin, and rifampicin, are bisubstrates for both OATP1B1 and OATP1B3 (Ishiguro et al., 2006). Therefore, the hepatic uptake of cationic and bulky compounds via hOCT1 and OATP1B1/1B3, respectively, in humans

DMD Fast Forward. Published on March 10, 2008 as DOI: 10.1124/dmd.108.020669
This article has not been copyedited and formatted. The final version may differ from this version.

seems likely. On the other hand, biliary excretion is also one of the major pathways for the elimination of compounds from blood circulation. Several kinds of ATP-binding cassette (ABC) transporters, such as multidrug resistance 1 (MDR1/Mdr1), multidrug resistance associated protein 2 (MRP2/Mrp2), and breast cancer resistance protein (BCRP/Bcrp) present on the canalicular membrane of the hepatocytes, play an important role in this biliary excretion in rats and humans (Tian et al., 2007, Matsushima et al., 2005). In general, MDR1/Mdr1 accepts hydrophobic cationic or neutral compounds preferentially, whereas MRP2/Mrp2 is responsible for the biliary excretion of a wide variety of organic anions, including glutathione and glucuronide conjugates, and BCRP/Bcrp accepts various kinds of organic anions and transports sulfate conjugates preferentially (Konig et al., 1999, Tanigawara, 2000, Suzuki et al, 2003).

The chemical structure of YM758 (M.W.: 567.54 as monophosphate salt) suggests that it is weakly basic (cationic) under physiological conditions and relatively bulky (Fig. 1). In this study, the transporters that contribute to the active hepatic uptake and excretion processes of YM758 in humans (and partially in rats) were clarified using several stably transporter-expressing mammalian cells and hepatocytes, with special focus on hOCT1/rOct1, OATP1B1, and OATP1B3 for the uptake process as well as MDR1 for excretion. Given that If channel inhibitors such as ivabradine have recently become a new class of agents for heart

disease, this study is valuable because it is the first to speculate on the transporter-mediated hepatic uptake and excretion of an If channel inhibitor.

Materials and Methods

Materials

[^{3}H]-MPP (specific radioactivity: 83,500 mCi/mmol) and [^{3}H]-$E_2$17βG (specific radioactivity: 53,000 mCi/mmol) were purchased from PerkinElmer Life Science Products, Inc. (Boston, MA, USA). [^{14}C]-Metformin hydrochloride (specific radioactivity: 54.0 mCi/mmol, radiochemical purity: 99.9%) was obtained from Moravek Biochemicals, Inc. (Brea, CA, USA). [^{14}C]-YM758 monophosphate (specific radioactivity: 2,750 mCi/mmol; radioactivity purity: 98.0%) was synthesized at Daiichi Pure Chemicals Co., Ltd. (Ibaraki, Japan). Cimetidine and sodium butyrate were obtained from Wako Pure Chemicals Industries, Ltd. (Osaka, Japan). Quinidine sulfate was purchased from Nacalai Tesque, Inc. (Kyoto, Japan). YM758 monophosphate and YM-344505 (d4-YM758 monophosphate), an internal standard for the analysis of YM758, were synthesized at the Process Chemistry Laboratories and Chemistry Laboratories of Astellas Pharmaceutical Inc., respectively (Ibaraki, Japan). Medium 199, gentamicin, and hygromycin B were obtained from Sigma-Aldrich (MO, USA). Fetal bovine serum (FBS) was purchased from Invitrogen (CA, USA) and JRH Biochemicals (KS, USA). Other materials used include Dulbecco's phosphate-buffered saline (PBS), 0.05% trypsin-EDTA solution,

penicillin-streptomycin, Dulbecco's modified eagle medium (DMEM), 10×Hank's balanced salt solution (HBSS) and Zeocin™, all from Invitrogen. All other chemicals and reagents were of analytical grade and purchased from commercial sources.

Construction of mammalian cells expressing hOCT1, rOct1, OATP1B1, and OATP1B3

The OATP1B1 and OATP1B3 cDNAs were cloned from human liver total RNA (Becton Dickinson, Heidelberg, Germany) using the RT-PCR method. Primers that are specific for OATP1B1 and OATP1B3 were designated on the basis of the sequence infomation of NM_006446 and NM_019844, respectively. The OATP1B1 cDNA was amplified using the forward primer-containing Nhe I site, 5'-gcgctagcatcatggaccaaaatcaacatttg-3', and the reverse primer-containing Not I site, 5'-atgcggccgctggaaacacagaagcagaagtg-3'. The PCR product was ligated into the pCR®4-TOPO vector system (Invitrogen), followed by subcloning into pcDNA3.1 (+), after which it was sequenced. Full length OATP1B1 was cut from pcDNA3.1(+) using NheI and NotI, and subcloned into pcDNA3.1/Zeo (+) (Invitrogen). The N-terminal fragment of OATP1B3 was amplified using the forward primer containing the BamH I site, 5'-aggatccatggaccaacatcaac-3', and the reverse primer, 5'-ggcaactgatttgctttcgc-3'. The C-terminal fragment was amplified using the forward primer, 5'-ggtcagtctgcatctcatgc-3', and the

reverse primer, 5'-attgtcagtgaaagaccagg-3'. Each PCR product was ligated into pGEM®-T Easy Vector Systems (Promega Corporation, Madison, WI, USA), followed by subcloning into pcDNA3.1/Zeo (+) (Invitrogen), and sequenced. The HEK293 cells (American Type Culture Collection CRL-1573), a transformed cell line derived from human embryo kidney, were cultured in complete medium consisting of DMEM with 10% fetal bovine serum and 1% penicillin-streptomycin in an atmosphere of 5% CO_2, 95% air at 37 °C. Each pcDNA3.1/Zeo (+) plasmid vector DNA containing OATP1B1 and OATP1B3 cDNA was purified using 100% ethanol containing sodium acetate. On the day before transfection, HEK293 cells were seeded onto poly-$_D$-lysine-coated 12-well plates (Becton Dickinson, Heidelberg, Germany) at a density of 0.5-1.0×10^5 cells/well. The cells were transfected with total DNA plasmid per well using Fugene6 (Roche) according to the manufacturer's instructions. The day after transfection (about 29 h after transfection), the medium was changed to the complete medium described above, which contained 200 μg/ml of Zeocin™. OATP1B1- and OATP1B3-expressing cells were then selected using Zeocin™. The expression of OATP1B1 and OATP1B3 in HEK293 cells was verified using real-time PCR, Western blot analysis. In addition, the great time-dependent uptake of $E_2$17βG which is a typical substrate for both OATP1B1 and OATP1B3 was confirmed in these expressing cells, whereas the uptake of $E_2$17βG into mock-HEK293 cells was much less

than that into the expressing cells. HEK293 cells stably expressing hOCT1 and rOct1, as well as negative control cells (mock-HEK293 cells), were constructed as described previously (Umehara *et al.* 2007a).

Uptake studies using mock, hOCT1, rOct1, OATP1B1, and OATP1B3-HEK293 cells

Transporter-expressing or vector-transfected HEK293 cells were grown in DMEM supplemented with 10% fetal bovine serum and 1% penicillin-streptomycin (v/v), and 100 μg/ml of Zeocin^{TM} at 37 °C in an atmosphere of 5% CO_2 and 95% humidity. The cells were subcultured in a medium containing 0.05% trypsin-EDTA solution. Cells were then seeded in poly-$_D$-lysine-coated 12-well plates at a density of 1.2×10^5 cells/well. For the transport study, the cell culture medium was replaced with culture medium supplemented with 5 mM sodium-butyrate for 24 h before the transport assay to induce the expression level of hOCT1, rOct1, OATP1B1, and OATP1B3. The transport study was performed as described previously (Umehara et al., 2007a). Uptake was initiated by adding Krebs-Henseleit buffer containing radio-labeled substrates {[^{3}H]-MPP (0.6 nM), [^{14}C]-metformin (10 μmol/l), [^{3}H]-$E_2$17βG (20 nM), or [^{14}C]-YM758 (10 μmol/l)} after the cells had been washed twice and pre-incubated with Krebs-Henseleit buffer at 37 °C for 15 min. In the concentration-dependent uptake and/or inhibition studies, the cells were incubated further in the presence of YM758 (1-1,000 μmol/l). The Krebs-Henseleit buffer

consisted of 2.0 mg/ml D-glucose, 0.141 mg/ml magnesium sulfate (anhydrous), 0.16 mg/ml potassium phosphate monobasic, 0.35 mg/ml potassium chloride, 6.9 mg/ml sodium chloride, 0.373 mg/ml of calcium chloride dihydrate, 1.5 mg/ml of HEPES and 2.1 mg/ml of sodium bicarbonate. The pH of this solution was adjusted to 7.4 with sodium hydroxide. The uptake was terminated at the designated time by adding ice-cold Krebs-Henseleit buffer after removing the incubation buffer. Then, the cells were washed twice with 1 ml of ice-cold Krebs-Henseleit buffer, solubilized in 0.5 ml of 1.0 mol/l sodium hydroxide, and kept overnight at 4 °C. Aliquots (0.5 ml) were transferred to scintillation vials after adding 0.25 ml of 2.0 mol/l hydrochloric acid. The radioactivity associated with the cells and incubation buffer was measured in a liquid scintillation counter (Tricarb-2700TR; PerkinElmer Life Science Products, Inc.) after adding 5 ml of scintillation fluid (Hionic Fluor; PerkinElmer Life Science Products, Inc.) to the scintillation vials. The remaining cell lysate was used to determine the protein concentration by the method of Lowry (Bio-Rad D_c Protein Assay; Bio-Rad Laboratories, Hercules, CA, USA), with bovine serum albumin as the standard.

Uptake studies using human hepatocytes

Cryopreserved human hepatocytes were purchased from Xenotech, LLC. (Lenexa, KS, USA).

In these experiments, three batches of human hepatocytes (Lots 639A, 653, and 549) that took up at least three times as much [^{3}H]-MPP during incubation at 37 °C than that at 4 °C under the linear conditions in the time-dependent uptake study, were selected as the positive control for further kinetic analyses. Just before the study, the hepatocyte suspension was thawed at 37 °C, quickly suspended in Tube A of the hepatocyte isolation kit (Xenotech, LLC.) containing DMEM and isotonic percoll, and then centrifuged (70 ×*g*) for 5 min at 20 °C. The supernatant was then removed, and the cells were resuspended in 4 ml of buffer from Tube B of the hepatocyte isolation kit, which contained supplemented DMEM. The number of viable cells was then determined using trypan blue staining. The cell viability ranged from 80% to 92% in human hepatocytes. Subsequently, the cryopreservation buffer was removed by resuspending the cells in the remaining buffer from Tube B (approximately 40 ml). The cells were then centrifuged (50 ×g) for 3 min at 20 °C, followed by removal of the supernatant. Finally, the cells were resuspended in the Krebs-Henseleit buffer at a density of 2.0×10^{6} viable cells/ml for the transport study. Prior to the uptake studies, the cell suspensions were pre-warmed in an incubator set at 37 °C for 3 min. The uptake studies were initiated by adding an equal volume of buffer containing labeled substrates {[^{14}C]-YM758 (10 μmol/l)} to the cell suspension. In the concentration-dependent uptake and/or inhibition studies, the cells were incubated further in the

presence of YM758 (1-1,000 μmol/l), cimetidine (10-10,000 μmol/l) or quinidine (1-1,000 μmol/l). The effect of the incubation temperature on the uptake of substrates was also investigated. After incubation at 37 °C or 4 °C for the designated time intervals, the reaction was terminated by separating the cells from the substrate solution. For this purpose, a 0.2 ml aliquot of incubation mixture was collected in a centrifuge tube containing 0.05 ml of 2 mol/l sodium hydroxide under a 0.1 ml layer of oil (a mixture of silicone oil and mineral oil; density: 1.015; Sigma-Aldrich). Subsequently, the sample tube was centrifuged for 10 sec using a tabletop centrifuge [10 000 ×g, centrifuge 5417C; Eppendorf AG (Hamburg Germany)]. During this process, the hepatocytes passed through the oil layer into the alkaline solution. After the hepatocytes were dissolved in the alkaline solution by incubating them overnight, the centrifuge tube was cut, and the contents of each compartment were transferred to separate scintillation vials. The contents of the compartment containing the dissolved cells were neutralized with 0.05 ml of 2 mol/l hydrochloric acid. The contents of each compartment were then mixed with scintillation cocktail in their respective vials, and the radioactivity in each was measured with a liquid scintillation counter.

Transcellular transport studies across LLC-PK1 and LLC-MDR1 cell monolayers

LLC-PK1 cells (porcine kidney epithelial LLC-PK1 cells transfected with only mock vectors) and MDR1-transfected LLC-PK1 cells (LLC-MDR1; LLC-PK1 cells transfected with vectors containing human MDR1 cDNA) were used at Daiichi Pure Chemicals Co., Ltd. under sublicense from BD Biosciences (CA USA). Prior to the assay, cells were cultured in 75cm^2 bottom flask (Falcon, NJ USA) and subjected to passage every 4 or 5 days. LLC-PK1 cells and MDR1 expressing cells were seeded at a density of 4×10^4 cells/insert in plates (Falcon). The cells were incubated in a CO_2 incubator (37 °C, CO_2: 5%) for 8 days to prepare cell monolayers for the determination of transcellular transport activity. Medium 199 containing 9% FBS, 50 μg/ml gentamicin, and 100 μg/ml hygromycin B were used for flask cultures. Only medium 199 containing 9% FBS and 50 μg/ml gentamicin was used for plate cultures. The transcellular transport studies using LLC-PK1 and LLC-MDR1 cells were performed according to a previous report (Adachi et al. 2001). The medium on the culture insert and plate seeded with cultured cells was removed by aspiration and replaced with HBSS, after which the cells were pre-incubated for 1 h at 37 °C. The medium on either the apical (100 μl) or basal (600 μl) side was replaced with HBSS solution containing the test substance (YM758), and the cells were then incubated at 37 °C. After incubation for 1, 2, and 4 h, 70 μl of HBSS was collected from the non-treated side to determine the transported amount of YM758. To compensate for the

collection volume, 70 μl of HBSS pre-warmed to 37 °C was added immediately. In the concentration-dependent transcellular transport studies, the cells (treated side only) were incubated further in the presence of YM758 (0.3-1,000 μmol/l).

Measurement method for determining YM758 concentrations in HBSS

Transcellular transport studies across LLC-PK1 and LLC-MDR1 cell monolayers were performed using non-labeled YM758 as the test substance. The peak areas of YM758 and its internal standard [YM-344540, deuterium (d4) labeled YM758 monophosphate] were analyzed using high-performance liquid chromatography with a tandem-mass spectrometry system. An API4000 with an atmosphere pressure ionization source (Applied Biosystems, CA, USA) was used. The atmosphere pressure ionization source was fitted with an electron spray ionization inlet to ionize the analytes. The electron spray voltage was set to 4.5 kV. In the positive ion mode, YM758 and its internal standard were subjected to multiple reaction monitoring, with transmitted molecular ions at *m/z* 470.5 and 474.2, respectively. These ions were subjected to collision-activated dissociation using argon, followed by monitoring of the product ions at *m/z* 166.3 and 170.3, respectively. Chromatographic separation was achieved using an XTerra MS C18 column (4.6×30 mm, 3.5 μm) (Waters, MA, USA), with a mobile phase of

acetonitrile/water/formic acid (40:60:0.1, v/v/v) at a flow rate of 0.25 ml/min. The standard curve for YM758 was linear from 0.001 to 1 μmol/l, and the correlation coefficient was >0.99. The accuracy of each concentration back-calculated from the regression equation was 87.4% to 109.0%.

Data analysis

Transport study using mock, hOCT1, rOct1, OATP1B1, and OATB1B3-HEK293 cells

YM758 uptake into transporters-expressing HEK293 cells and vector-transfected HEK293 cells was expressed as the uptake volume (μl/mg protein) (amount of radioactivity in the cells divided by its concentration in the incubation medium). In this study, the time-dependent uptake of [^{14}C]-YM758 (10 μmol/l) for mock, rOct1, hOCT1, OATP1B1, and OATP1B3-HEK293 cells at 0.25, 0.5, 1, 2, 3, 5, 10, and 15 min after the initiation of incubation was determined. The uptake time span, during which transport activity was linear, was determined only for the uptake of [^{14}C]-YM758 into mock-HEK293 cells. Subsequently, the concentration-dependence of the [^{14}C]-YM758 uptake clearance was evaluated for mock cells at the designated time mentioned above. The kinetic parameters were estimated using Michaelis-Menten plots based on the following equation:

DMD Fast Forward. Published on March 10, 2008 as DOI: 10.1124/dmd.108.020669
This article has not been copyedited and formatted. The final version may differ from this version.

$$v/S = V_{max}/(K_m+S) + P_{dif} \quad (1)$$

where v/S is the initial uptake clearance of the substrate (μl/min/mg protein), S is the substrate concentration in the medium (μmol/l), K_m is the Michaelis-Menten constant (μmol/l), and V_{max} is the maximum uptake rate (nmol/min/mg protein). P_{dif} represents the non-saturable uptake clearance (μl/min/mg protein). Fitting was performed using the nonlinear least-squares method and WinNonlin (Pharsight Corporation). The uptake of [^{3}H]-MPP, [^{14}C]-metformin, and [^{3}H]-$E_2$17βG into rOct1, hOCT1, and OATP1B1 and OATP1B3-expressing HEK293 cells in the presence of inhibitors (non-radiolabeled YM758) was examined at 1, 5, and 2 min, respectively, for each substrate. The times were decided in accordance with the information in the literature (Umehara et al., 2007a, 2007b).

Transport study using human cryopreserved hepatocytes

The uptake of [^{14}C]-YM758 into human hepatocytes was expressed as the uptake volume (μl/10^6 cells) [amount taken up into cells (pmol/10^6 cells) divided by the concentration of radioactivity in the incubation medium (pmol/μl)]. First, the time-dependent uptake of [^{14}C]-YM758 (10 μmol/l) into hepatocytes at 1, 5, 10, and 30 min at 37 °C was investigated in order to determine how long transport activity was linear. The kinetic analysis of the

concentration-dependent ligand uptake was performed for human hepatocytes using WinNonlin and the following equations, which assume that the ligands are transported via one saturable carrier-mediated component and one linear passive one:

$$v/S = V_{max}/(K_m+S) + P_{dif} \quad (2)$$

where v/S is the uptake clearance of the substrate (μl/min/10^6 cells), S is the substrate concentration in the medium (μmol/l), K_m is the Michaelis-Menten constant (μmol/l), and V_{max} is the maximum uptake rate (pmol/min/10^6 cells). P_{dif} represents the non-saturable uptake clearance (μl/min/10^6 cells). The uptake of [^{14}C]-YM758 into human hepatocytes in the presence of inhibitors (non-radiolabeled YM758, cimetidine, and quinidine) was examined at 1 min.

Inhibition study in hOCT1/rOct1, OATP1B1/OATP1B3-expressing cells, and hepatocytes

The inhibitory effects of non-radiolabeled YM758 (1-1,000 μmol/l) on the uptake of [^{3}H]-MPP (1.2 or 0.6 nM), [^{14}C]-metformin (10 μmol/l), and [^{3}H]-$E_2$17βG (20 nM) for rOct1, hOCT1, and OATP1B1 and OATP1B3, as well as those of cimetidine (10-10,000 μmol/l) and quinidine (1-1,000 μmol/l) on the uptake of [^{14}C]-YM758 (10 μmol/l) were investigated, and the IC_{50} value for each inhibitor was estimated. For the inhibition study, the transfected cells and/or

DMD Fast Forward. Published on March 10, 2008 as DOI: 10.1124/dmd.108.020669
This article has not been copyedited and formatted. The final version may differ from this version.

hepatocytes were incubated with incubation buffer containing each substrate and inhibitor at several concentrations while the linearity of the uptake activity was maintained. The other procedures were performed in the same way as the uptake studies. For the calculation of the IC_{50} values, the Hill equation was fitted to the data using WinNonlin and the following equation:

$$v = v_0/[1+(I/IC_{50})] \quad (3)$$

where v is the uptake rate of each substrate in the presence of the inhibitor, v_0 is the uptake rate of each substrate in the absence of the inhibitor, and I is the concentration of the inhibitor.

Transcellular transport study in LLC-PK1 and LLC-MDR1 cells

In the transcellular transport study of YM758 using LLC-PK1 and LLC-MDR1 cells, the permeability-surface area (PS) product across the monolayer was defined as follows:

$$\text{PS product}=A/t/C_0 \quad (4)$$

where t, A, and C_0 represent the incubation time, the amount of compound transported per well of cell monolayer, and the initial concentration of compounds on the donor side, respectively. The flux ratio (μl/well) across the monolayer was defined as

$$\text{Flux ratio}=PS_{b\ to\ a}/PS_{a\ to\ b} \quad (5)$$

where $PS_{b\ to\ a}$ and $PS_{a\ to\ b}$ represent the PS product in the basal to apical direction and the apical

to basal direction, respectively. In LLC-PK1/LLC-MDR1 cells, the corrected flux ratio was defined by the following equation:

Corrected flux ratio=(flux ratio in LLC-MDR1 cells)/(flux ratio in LLC-PK1 cells) (6)

In this study, the concentration-dependent transcellular transport of YM758 in LLC-PK1 and LLC-MDR1 cells was investigated at various YM758 concentrations (0.3-1,000 μmol/l). The K_m value of YM758 was calculated from the relationship between the corrected flux ratio and the concentration of test substance using WinNonlin software according to the Michaelis-Menten equation as follows:

$$\text{Corrected flux ratio} = 1 + [(V_{max}/PS_2)/(K_m+S)] \quad (7)$$

where S, PS_2, and K_m represent the YM758 concentration, efflux clearance mediated by passive diffusion on apical cell surface, and Michaelis-Menten constant (μmol/l), respectively.

Statistical Analysis

Each uptake experiment was done in triplicate, and the results are given as the mean ± S.D., except for the time-dependent uptake study for hepatocytes (n=2).

Results

Uptake and Inhibition Profile of YM758 for Mock and rOct1/hOCT1-HEK293 Cells

First, the time-dependent uptake of [^{14}C]-YM758 into mock- and rOct1/hOCT1-HEK293 cells was investigated. The high uptake volume of [^{14}C]-YM758 into rOct1/hOCT1-HEK293 cells, ranged from 300 to 400 μl/mg protein at 15 min, whereas the time-dependent uptake of this compound into mock-HEK293 cells was also extremely high, which suggests that the uptake for [^{14}C]-YM758 via rOct1 or hOCT1 was slight, if at all (Fig.2). The concentration-dependent uptake of [^{14}C]-YM758 into mock-HEK293 cells was determined at the earliest time practically and technically possible (3 min). The uptake of [^{14}C]-YM758 was saturable in mock-HEK293 cells with K_m, V_{max}, V_{max}/K_m, and P_{dif} values of 135 μmol/l, 6.43 nmol/min/mg protein, 47.7 μl/min/mg protein, and 6.80 μl/min/mg protein, respectively (Fig. 3).

The inhibitory effect of YM758 on [^{3}H]-MPP uptake via rOct1 and hOCT1 was also investigated. As shown in Fig. 4, YM758 inhibited rOct1- and hOCT1-mediated [^{3}H]-MPP uptake in a concentration-dependent manner with IC_{50} values of 23.8 μmol/l and 40.5 μmol/l, respectively. The IC_{50} value of YM758 for [^{14}C]-metformin uptake via rOct1 may be estimated below 10 μmol/l in the same way as described above, whereas that was much smaller than that

for [^{3}H]-MPP uptake.

Uptake and Inhibition Profile of YM758 for OATP1B1 and OATP1B3-HEK293 Cells

The time-dependent uptake of [^{14}C]-YM758 into OATP1B1 and OATP1B3-HEK293 cells was also investigated. The uptake of [^{14}C]-YM758 was greater in OATP1B1-HEK293 than that in mock-HEK293 (Fig. 5). No difference in the uptake of [^{14}C]-YM758 into OATP1B3-HEK293 cells and mock-HEK293 cells was observed.

In addition, the inhibitory effect of YM758 on [^{3}H]-$E_2$17βG uptake via OATP1B1 and OATP1B3 was investigated. As shown in Fig. 6, YM758 inhibited OATP1B1-mediated [^{3}H]-$E_2$17βG uptake in a concentration-dependent manner with a IC_{50} value of 13.0 μmol/l. YM758 had no inhibitory effect on OATP1B3-mediated [^{3}H]-$E_2$17βG uptake.

Uptake and Inhibition Profile of YM758 for Human Cryopreserved Hepatocytes

The time profiles for the uptake of [^{14}C]-YM758 in human hepatocytes are shown in Fig. 7. The uptake of YM758 was higher at 37 °C than at 4 °C in human hepatocytes, which suggests that [^{14}C]-YM758 is taken up into hepatocytes via an active transport mechanism. The similar experiments were performed with rat hepatocytes but the results were not meaningful likely to

DMD Fast Forward. Published on March 10, 2008 as DOI: 10.1124/dmd.108.020669
This article has not been copyedited and formatted. The final version may differ from this version.

their poor viability (67-76%) (data not shown). The concentration-dependent uptake of [^{14}C]-YM758 into human hepatocytes was investigated as shown in Fig. 8 (A) at the earliest time practically and technically possible (1 min), but the same type of uptake study using rat hepatocytes was not performed. The saturable uptake of [^{14}C]-YM758 into human hepatocytes was observed with K_m, V_{max}, V_{max}/K_m, and P_{dif} values of 87.9 μmol/l, 2590 pmol/min/10^6 cells, 29.5 μl/min/10^6 cells, and 23.7 μl/min/10^6 cells, respectively.

In addition, the inhibitory effect of cimetidine and quinidine on [^{14}C]-YM758 uptake into human hepatocytes was also investigated. As shown in Fig. 8 [(B) and (C)], quinidine inhibited [^{14}C]-YM758 uptake into human hepatocytes with IC_{50} value of 147 μmol/l whereas this uptake was not inhibited in the presence of 10,000 μmol/l of cimetidine.

Transcellular Transport of YM758 across MDR1-transfected LLC-PK1 Cells

The permeation clearance for basal-to-apical flux and apical-to-basal flux of YM758 across LLC-PK1 and LLC-MDR1 monolayers are shown in Fig. 9 [(A) and (B)]. The permeation clearance ratios, the permeation clearance from the basal to apical side divided by that of the opposite direction, were almost constant (1.2-1.5) in LLC-PK1 cells, irrespective of the YM758 concentrations in the range of 0.3 to 1000 μmol/l. On the other hand, the permeation clearance

DMD Fast Forward. Published on March 10, 2008 as DOI: 10.1124/dmd.108.020669
This article has not been copyedited and formatted. The final version may differ from this version.

ratios in LLC-MDR1 cells were 21.8, 16.9, 16.7, 12.6, 13.1, 4.5, 2.1, and 1.5 in the presence of 0.3, 1, 3, 10, 30, 100, 300 and 1000 μmol/l of YM758, respectively. This suggests that YM758, like quinidine and digoxin, is a typical substrate for MDR1 because the basal-to-apical flux markedly exceeded that of the apical-to-basal flux in LLC-MDR1 cells. The relationships between the YM758 concentrations and corrected flux ratios, which were obtained by dividing the permeation clearance ratios in LLC-MDR1 cells by those in LLC-PK1 cells, are presented in Fig. 9 (C). This result also indicates that YM758 is a MDR1 substrate with a K_m value of 20.9 μmol/l.

Discussion

In general, the drug elimination pathway from the liver is composed of three main processes, which are passive or active uptake from systemic circulation into hepatocytes, metabolism/conjugation mediated by CYP and other types of enzymes, and passive or active excretion into the bile. In this study, the active hepatic uptake and excretion of YM758, a novel If channel inhibitor, were clarified using several transporter-expressing mammalian cells and hepatocytes. This is the first case in which the transporter-mediated hepatic uptake and excretion of an If channel inhibitor was investigated. The obtained K_m and IC_{50} values for the concentration-dependent uptake and inhibition profile of YM758 in this study were all summarized in Table 1.

Several cationic (basic) compounds such as MPP, TEA, cimetidine and metformin are substrates of hOCT1 and rOct1, which are mainly expressed in the basal membrane of hepatocytes in humans and rats, respectively (Zhang et al., 1997; Grundemann et al., 1999, 2003; Dudley et al., 2000; Wu et al., 2000; Gorboulev et al., 1997, 1999; Arndt et al., 2001; Sakata et al., 2004; Urakami et al., 1998, 2002, Kimura et al., 2005). It was also reported that the genetic variation of hOCT1 may affect the pharmacokinetics of metformin, an anti-diabetic reagent, in

humans (Shu et al., 2007). This information suggests that hOCT1/rOct1-mediated uptake into hepatocytes may be an important determinant of the pharmacokinetics of cationic drugs. Therefore, the time-dependent uptake of YM758 into hOCT1/rOct1-HEK293 cells (Fig. 2) was first investigated because YM758 is a weakly basic compound (pKa value: 8.02). In this study, YM758 was taken up into hOCT1/rOct1-HEK293 cells only slightly, compared with the uptake into mock-HEK293 cells.

On the other hand, several bulky and hydrophobic compounds such as pravastatin, pitavastatin, valsaltan, telmisartan, and temocapril are known to be OATP1B1 and OATP1B3 substrates, which are predominantly expressed on the basal side of hepatocytes in humans (Maeda et al., 2006, Yamashiro et al., 2006, Ishiguro et al., 2006, Hirano et al., 2006). In the present study, the uptake of YM758 into OATP1B1- and OATP1B3-HEK293 cells was also evaluated because the structure of YM758 is relatively bulky. As shown in Fig. 5, the uptake of YM758 via OATP1B1 was greater than that into mock-HEK293 cells, whereas that via OATP1B3 was not. This suggests that YM758 may be mainly taken up into human hepatocytes via an OATP1B1-mediated uptake mechanism. In addition, the inhibitory effect of YM758 on the uptake of $E_2$17βG, which is one of the typical substrates both for OATP1B1 and OATP1B3, was investigated using these transporter-expressing HEK293 cells. YM758 was shown to be effective as an inhibitor for

OATP1B1, but not OATP1B3, because the inhibition curve was obtained only from OATP1B1-HEK293 cells (IC_{50} value: 13.0 μmol/l) (Fig. 6).

The hepatic uptake mechanism of YM758 was clarified using human hepatocytes, and the uptake of YM758 into hepatocytes at 37 °C was higher than that at 4 °C in humans (Fig. 7), which suggests the existence of an active transport mechanism for YM758 in hepatocytes. Because the uptake of YM758 into rat hepatocytes was not meaningful due to their poor viability (67-76%) (data not shown), the concentration-dependent uptake of YM758 and the inhibitory effect of inhibitors for hOCT1 and OATP1B1 on YM758 uptake were examined using human hepatocytes (Figs. 7 and 8). The uptake of YM758 into human hepatocytes was concentration-dependent, with a K_m value of 87.9 μmol/l. This affinity is not comparable to the IC_{50} value for YM758 on $E_2$17βG uptake into OATP1B1-HEK293 cells (13.0 μmol/l), which suggests that YM758 may not be a competitive inhibitor for OATP1B1. For rOatp2, which is a counterpart molecule for OATP1B1 in rats, several active transport sites in the molecules were speculated in transport studies using several substrates and inhibitors ($E_2$17βG, digoxin, and taurocholate) (Sugiyama et al., 2002). The difference between the YM758 K_m and IC_{50} values obtained for OATP1B1-HEK293 cells and human hepatocytes may be due to several active transport sites in the OATP1B1 molecule, although further investigation is required. In addition,

for YM758's concentration-dependent uptake profile in human hepatocytes, the clearance corresponding to the non-saturable component was estimated to be 23.7 μl/min/10^6 cells, which is a larger value than those (approx. 5.0 μl/min/10^6 cells) for other cationic compounds, such as MPP, TEA, and cimetidine (Umehara et al., 2007b).

In Fig. 8, the inhibitory effects of cimetidine and quinidine on YM758 uptake into human hepatocytes are presented. Cimetidine is a typical inhibitor for hOCT1, which is only the OCT family expressed in the basal membrane of human hepatocytes. Cimetidine did not inhibit YM758 uptake into human hepatocytes (Fig. 8B), which suggests that YM758 may not be taken up into human hepatocytes via hOCT1, but actually works as a hOCT1 inhibitor (Fig. 4A). The fact that YM758 uptake into hOCT1-HEK293 cells was only marginal supports this hypothesis. In contrast, quinidine inhibited YM758 uptake into human hepatocytes in a concentration-dependent manner, with a IC_{50} value of 147 μmol/l. In oocyte studies, the uptake activity of an opioid peptide analogue via OATP1B1 in the presence of 500 μmol/l quinidine was inhibited at a level of only 80% of the control values (Nozawa et al., 2003). Quinidine is also known as a typical inhibitor for hOCT1 and MDR1 with IC_{50} values of 16.0 μmol/l (figure not shown) and 13.2 μmol/l (Storch et al., 2007), respectively. The inhibition constant for hOCT1 and MDR1 may be much smaller than that for OATP1B1, and YM758 uptake into human

hepatocytes is not inhibited in the presence of lower concentrations of quinidine which works as a inhibitor for hOCT1 and MDR1. These results revealed that YM758 may be taken up into human hepatocytes via OATP1B1, but not via hOCT1.

The uptake volume of YM758 in mock-HEK293 cells was 200-300 μl/mg protein after 15-min incubation, and the uptake of YM758 into mock-HEK293 cells was concentration-dependent (Fig. 3). The endogenous expression of several ion channels and receptors in HEK293 cells has been already reported (Gunthorpe et al., 2001) whereas there are no information on that of transporters in this cell line. It may be necessary to identify the basal expression of transporters in HEK293 cells for the investigation of the active transport of new chemical entities. In addition, as discussed above, the non-saturable component of the uptake of YM758 into human hepatocytes were larger than that of several cationic compounds at 4°C. Considering the extensive uptake of YM758 into mock-HEK293, there seem to be a small contribution of unknown uptake mechanisms to the total uptake of YM758, which might be likely those in HEK293 cells, in human hepatocytes.

In the transcellular transport study using LLC-PK1 and LLC-MDR1 cells, the saturable transport of YM758 via MDR1 was observed, which suggests that YM758 may be excreted into the bile via MDR1 in the human liver (Fig. 9). A schematic diagram illustrating YM758

elimination mechanism in the human liver that was deduced from the results of all these studies is shown in Fig. 10. YM758 may be taken up into human hepatocytes mainly via OATP1B1, rather than hOCT1, and presumably via unknown uptake processes or passive diffusion. After that, it may be subject to metabolism and/or conjugation, or excreted into the bile via MDR1. This type of hepatic elimination mechanism is also reported in the case of fexofenadine, which is taken up via the OATP family and is excreted into the bile via MDR1 (Cvetkovic et al., 1999). The transporters associated with the elimination of YM758 from human hepatocytes may correspond to those in rats, although further investigation is required.

Recently, new chemical entities that may undergo extensive metabolism by CYP enzymes or those that may have a significant inhibitory effect on CYP-mediated metabolism are being dropped at the drug screening stage. These trends will eventually result in an increase in the number of drug candidates eliminated exclusively by Phase II enzymes and/or transporters. Therefore, it is important to estimate the transporter-mediated hepatic uptake and excretion pathway of new chemical entities. These types of studies, which focus on emerging therapeutic drugs with new pharmacological actions, will have a large impact on future pharmacokinetic research.

References

Adachi Y, Suzuki H, Sugiyama Y (2001) Comparative studies on in vitro methods for evaluating in vivo function of MDR1 P-glycoprotein. *Pharm Res* 18:1660-1668.

Arndt P, Volk C, Gorboulev V, Budiman T, Popp C, Ulzheimer-Teuber I, Akhoundova A, Koppatz S, Bamberg E, Nagel G and Koepsell H (2001) Interaction of cations, anions, and weak base quinine with rat renal cation transporter rOCT2 compared with rOCT1. *Am J Physiol Renal Physiol* 281: F454-468.

Bucchi A, Barbuti A, Baruscotti M, DiFrancesco D (2007) Heart rate reduction via selective 'funny' channel blockers. *Curr Opin Pharmacol* 7: 208-213.

Buckberg GD, Fixler DE, Archie JP, Hoffman JI (1972) Experimental subendocardial ischemia in dogs with normal coronary arteries. *Circ Res* 30: 67-81.

Cvetkovic M, Leake B, Fromm MF, Wilkinson GR, Kim RB (1999) OATP and P-glycoprotein transporters mediate the cellular uptake and excretion of fexofenadine. *Drug Metab Dispos* 27:

866-871.

Dudley AJ, Bleasby K and Brown CD (2000) The organic cation transporter OCT2 mediates the uptake of beta-adrenoceptor antagonists across the apical membrane of renal LLC-PK(1) cell monolayers. *Br J Pharmacol* 131: 71-79.

Gorboulev V, Ulzheimer JC, Akhoundova A, Ulzheimer-Teuber I, Karbach U, Quester S, Baumann C, Lang F, Busch AE and Koepsell H (1997) Cloning and characterization of two human polyspecific organic cation transporters. *DNA Cell Biol* 16: 871-881

Gorboulev V, Volk C, Arndt P, Akhoundova A and Koepsell H (1999) Selectivity of the polyspecific cation transporter rOCT1 is changed by mutation of aspartate 475 to glutamate. *Mol Pharmacol* 56: 1254-1261.

Grundemann D, Liebich G, Kiefer N, Koster S and Schomig E (1999) Selective substrates for non-neuronal monoamine transporters. *Mol Pharmacol* 56: 1-10.

Grundemann D, Hahne C, Berkels R and Schomig E (2003) Agmatine is efficiently transported by non-neuronal monoamine transporters extraneuronal monoamine transporter (EMT) and organic cation transporter 2 (OCT2). *J Pharmacol Exp Ther* 304: 810-817.

Gunthorpe MJ, Smith GD, Davis JB, Randall AD (2001) Characterisation of a human acid-sensing ion channel (hASIC1a) endogenously expressed in HEK293 cells. *Pflugers Arch* 442: 668-674.

Hirano M, Maeda K, Shitara Y, Sugiyama Y (2006) Drug-drug interaction between pitavastatin and various drugs via OATP1B1. *Drug Metab Dispos* 34: 1229-1236.

Indolfi C, Guth BD, Miura T, Miyazaki S, Schulz R, Ross J Jr (1989) Mechanisms of improved ischemic regional dysfunction by bradycardia. Studies on UL-FS 49 in swine. *Circulation* 80: 983-993.

Ishiguro N, Maeda K, Kishimoto W, Saito A, Harada A, Ebner T, Roth W, Igarashi T, Sugiyama Y (2006) Predominant contribution of OATP1B3 to the hepatic uptake of telmisartan, an

angiotensin II receptor antagonist, in humans. *Drug Metab Dispos* 34: 1109-1115.

Kimura N, Masuda S, Tanihara Y, Ueo H, Okuda M, Katsura T and Inui K (2005) Metformin is a superior substrate for renal organic cation transporter OCT2 rather than hepatic OCT1. *Drug Metab. Pharmacokinet* **20**: 379-386.

Koepsell H, Schmitt BM, Gorboulev V 2003. Organic cation transporters. *Rev Physiol Biochem Pharmacol* 150: 36-90.

König J, Nies AT, Cui Y, Leier I, Keppler D (1999) Conjugate export pumps of the multidrug resistance protein (MRP) family: localization, substrate specificity, and MRP2-mediated drug resistance. *Biochim Biophys Acta* 1461: 377-394.

Laurent D, Bolene-Williams C, Williams FL, Katz LN (1956) Effects of heart rate on coronary flow and cardiac oxygen consumption. *Am J Physiol* 185: 355-364.

Maeda K, Ieiri I, Yasuda K, Fujino A, Fujiwara H, Otsubo K, Hirano M, Watanabe T, Kitamura Y,

Kusuhara H, Sugiyama Y (2006) Effects of organic anion transporting polypeptide 1B1 haplotype on pharmacokinetics of pravastatin, valsartan, and temocapril. *Clin Pharmacol Ther* 79: 427-439.

Matsushima S, Maeda K, Kondo C, Hirano M, Sasaki M, Suzuki H, Sugiyama Y (2005) Identification of the hepatic efflux transporters of organic anions using double-transfected Madin-Darby canine kidney II cells expressing human organic anion-transporting polypeptide 1B1 (OATP1B1)/multidrug resistance-associated protein 2, OATP1B1/multidrug resistance 1, and OATP1B1/breast cancer resistance protein. *J Pharmacol Exp Ther* 314: 1059-1067.

Muller M, Jansen PL (1997) Molecular aspects of hepatobiliary transport. *Am J Physiol* 272: G1285-1303.

Nozawa T, Tamai I, Sai Y, Nezu J, Tsuji A (2003) Contribution of organic anion transporting polypeptide OATP-C to hepatic elimination of the opioid pentapeptide analogue [D-Ala2, D-Leu5]-enkephalin. *J Pharm Pharmacol* 55: 1013-1020.

Opie L (1989) Trial alert. *Cardiovasc Drugs Ther* 3: 795-796.

Roth W, Bauer E, Heinzel G, Cornelissen PJ, van Tol RG, Jonkman JH, Zuiderwijk PB (1993) Zatebradine: pharmacokinetics of a novel heart-rate-lowering agent after intravenous infusion and oral administration to healthy subjects. *J Pharm Sci* 82: 99-106.

Sakata T, Anzai N, Shin HJ, Noshiro R, Hirata T, Yokoyama H, Kanai Y and Endou H (2004) Novel single nucleotide polymorphisms of organic cation transporter 1 (SLC22A1) affecting transport functions. *Biochem Biophys Res Commun* 313: 789-793.

Shu Y, Brown C, Castro RA, Shi RJ, Lin ET, Owen RP, Sheardown SA, Yue L, Burchard EG, Brett CM, Giacomini KM (2007) Effect of Genetic Variation in the Organic Cation Transporter 1, OCT1, on Metformin Pharmacokinetics. *Clin Pharmacol Ther*: Epub ahead of print

Sonnenblick EH, Ross J Jr, Braunwald E (1968) Oxygen consumption of the heart. Newer concepts of its multifactoral determination. *Am J Cardiol* 22: 328-336.

Storch CH, Theile D, Lindenmaier H, Haefeli WE, Weiss J (2007) Comparison of the inhibitory

activity of anti-HIV drugs on P-glycoprotein. *Biochem Pharmacol* 73: 1573-1581.

Sugiyama D, Kusuhara H, Shitara Y, Abe T, Sugiyama Y (2002) Effect of 17 beta-estradiol-D-17 beta-glucuronide on the rat organic anion transporting polypeptide 2-mediated transport differs depending on substrates. *Drug Metab Dispos* 30: 220-223.

Suzuki M, Suzuki H, Sugimoto Y, Sugiyama Y (2000) ABCG2 transports sulfated conjugates of steroids and xenobiotics. *J Biol Chem* 278: 22644-22649.

Tanigawara Y (2000) Role of P-glycoprotein in drug disposition. *Ther Drug Monit* 22:137-140.

Tian X, Li J, Zamek-Gliszczynski MJ, Bridges AS, Zhang P, Patel NJ, Raub TJ, Pollack GM, Brouwer KL (2007) Roles of P-glycoprotein, Bcrp, and Mrp2 in biliary excretion of spiramycin in mice. *Antimicrob Agents Chemother* 51: 3230-3234.

Umehara KI, Iwatsubo T, Noguchi K, Kamimura H (2007a) Comparison of kinetic characteristics of inhibitory effects by biguanides and H_2-blockers on the organic cation transporters-mediated

transport between human (OCT) and rat (oct): Insight into the application to the development of drug candidates. *Xenobiotica* 37: 618-634.

Umehara KI, Iwatsubo T, Noguchi K, Kamimura H (2007b) Functional involvement of organic cation transporter 1 (OCT1/Oct1) in the hepatic uptake of organic cations in humans and rats. *Xenobiotica* 37: 818-831.

Urakami Y, Okuda M, Masuda S, Saito H and Inui KI (1998) Functional characteristics and membrane localization of rat multispecific organic cation transporters, OCT1 and OCT2, mediating tubular secretion of cationic drugs. *J Pharmacol Exp Ther* 287: 800-805.

Urakami Y, Akazawa M, Saito H, Okuda M and Inui K (2002) cDNA cloning, functional characterization, and tissue distribution of an alternatively spliced variant of organic cation transporter hOCT2 predominantly expressed in the human kidney. *J Am Soc Nephrol* 13: 1703-1710.

Wu X, Huang W, Ganapathy ME, Wang H, Kekuda R, Conway SJ, Leibach FH and Ganapathy V

(2000) Structure, function, and regional distribution of the organic cation transporter OCT3 in the kidney. *Am J Physiol Renal Physiol* 279: F449-458.

Yamashiro W, Maeda K, Hirouchi M, Adachi Y, Hu Z, Sugiyama Y (2006) Involvement of transporters in the hepatic uptake and biliary excretion of valsartan, a selective antagonist of the angiotensin II AT1-receptor, in humans. *Drug Metab Dispos* 34: 1247-1254.

Yamazaki M, Suzuki H, Sugiyama Y (1996) Recent advances in carrier-mediated hepatic uptake and biliary excretion of xenobiotics. *Pharm Res* 13: 497-513.

Zhang L, Dresser MJ, Gray AT, Yost SC, Terashita S and Giacomini KM (1997) Cloning and functional expression of a human liver organic cation transporter. *Mol Pharmacol* 51: 913-921.

Footnotes

b) The name and full address of person to receive reprint requests

Name: Ken-ichi Umehara

Address: Drug Metabolism Research Laboratories, Drug Discovery Research,

Astellas Pharma Inc., 1-8, Azusawa 1-chome, Itabashi-ku,

Tokyo 174-8511, Japan

E-mail: kenichi.umehara@jp.astellas.com

Legends for figures

Fig. 1 Chemical structures of YM758 monophosphate (A) and ivabradine hydrochloride (B).

Fig. 2 Uptake of YM758 into rOct1-HEK293 (A) and hOCT1-HEK293 (B) cells.

The uptake of [^{14}C]-YM758 into hOCT1 (closed circle), rOct1 (open circle), and vector-HEK293 (open diamond) cells was determined. The uptake was initiated by adding ligand {[^{14}C]-YM758 (10 μmol/l)} and terminated at designated times by adding ice-cold buffer. The uptake value was normalized by the division of the cellular uptake amounts of the ligand by the ligand concentration in the medium. Each point represents the mean ± S.D. (n=3).

Fig. 3 Concentration-dependence of the uptake of YM758 into mock-HEK293.

The cellular uptake rates of [^{14}C]-YM758 into mock-HEK293 were determined at different substrate concentrations. The concentration-dependence of YM758 uptake into mock-HEK293 cells is shown by the Michaelis-Menten plots. Kinetic analyses revealed that the uptake of [^{14}C]-YM758 consists of one saturable and one non-saturable component and follows the Michaelis-Menten equation. The solid line represents the fitted line obtained by nonlinear regression analysis. Each point represents the mean ± S.D. (n=3).

Fig. 4 The inhibitory effect of YM758 on the uptake of MPP (A) and metformin (B) by hOCT1 and rOct1.

The uptake rates of [^{3}H]-MPP (0.6 or 1.2 nM) by hOCT1/rOct1 and those of [^{14}C]-metformin (10 μmol/l) by rOct1 were determined for 1 and 3 min, respectively, in the presence or absence of YM758 at the concentrations indicated. The closed and open circles represent hOCT1 and rOct1, respectively. The lines represent the fitted line obtained by nonlinear regression analysis. The details of the fitting procedure are described under *Materials and Methods.* Each point represents the mean ± S.D. (n=3).

Fig. 5 Uptake of YM758 into OATP1B1-HEK293 (A) and OATP1B3-HEK293 (B).

The uptake of [^{14}C]-YM758 into OATP1B1 (open circle), OATP1B3 (open triangle), and vector-HEK293 (open diamond) was determined. The uptake was initiated by adding ligand {[^{14}C]-YM758 (10 μmol/l)} and terminated at designated times by adding ice-cold buffer. The uptake value was normalized by dividing the amounts of ligand taken up by the cell by the ligand concentration in the medium. Each point represents the mean ± S.D. (n=3).

Fig. 6 The inhibitory effect of YM758 on the uptake of $E_2$17βG by OATP1B1 (A) and

OATP1B3 (B).

The uptake rates of [^{3}H]-$E_2$17βG (20 nM) by OATP1B1 and OATP1B3 were determined for 2 and 5 min, respectively, in the presence or absence of YM758 at the concentrations indicated. The open circles and triangles represent OATP1B1 and OATP1B3, respectively. The lines represent the fitted line obtained by nonlinear regression analysis. The details of the fitting procedure are described under *Materials and Methods.* Each point represents the mean ± S.D. (n=3).

Fig. 7 Time profiles for the uptake of YM758 into human hepatocytes at 37 °C and 4 °C.

The uptake of [^{14}C]-YM758 during 1, 5, 10, and 30 min was determined at 37 °C (closed circles), and 4 °C (open diamond). The uptake was initiated by adding ligands and terminated at designated times by separating the cells from the substrate solution using a tabletop centrifuge. Each point represents the average value from two determinations.

Fig. 8 The inhibitory effect of YM758 (A), cimetidine (B), and quinidine (C) on the uptake of [^{14}C]-YM758 into human hepatocytes.

The uptake rates of [^{14}C]-YM758 (10 μmol/l) into human hepatocytes were determined for 1 min.

In panel (A), kinetic analyses revealed that the uptake of [^{14}C]-YM758 consists of one saturable component, which follows the Michaelis-Menten equation (uptake at 37 °C; closed circles), and one non-saturable component (uptake at 4 °C; open diamonds). The solid and dotted lines represent the fitted lines obtained for the saturable and non-saturable components, respectively, using nonlinear regression analysis. In panels (B) and (C), the open circles and triangles represent the uptake of [^{14}C]-YM758 in the presence or absence, respectively, of cimetidine and quinidine at the concentrations indicated. The lines also represent the fitted line obtained by nonlinear regression analysis. The details of the fitting procedure are described under *Materials and Methods*. Each point represents the mean ± S.D. (n=3).

Fig. 9 Concentration-dependent profiles for the transcellular transport of YM758 across LLC-PK1 and LLC-MDR1 monolayers.

In panels (A) and (B), the permeation clearance of YM758 (0.3-1,000 μmol/l) across LLC-PK1 and LLC-MDR1 monolayers was determined. The ordinate represents the clearance (μl/well/h), which was calculated as the amount of each ligand transferred to the acceptor side divided by the initial concentration on the donor side, and the incubation time (4 h). The open and closed symbols represent the permeation clearances for basal-to-apical flux and apical-to-basal flux,

respectively. Panel (C) shows the corrected flux ratio of YM758 as a function of concentration. Kinetic analyses revealed that this corrected flux ratio consists of one saturable component, which follows the Michaelis-Menten equation, and was determined from the permeation clearance ratio of YM758 across LLC-PK1 and LLC-MDR1 cells during 4 h. The closed symbols represent the observed values. The line was fitted using nonlinear regression analysis, the details of which are described under *Materials and Methods*. Each point represents the mean ± S.D. (n=3).

Fig. 10 Schematic diagram illustrating the presumed elimination process of YM758 in human hepatocytes.

The solid and broken arrows represent the presumed elimination process of the unchanged drug (YM758) and its possible metabolites, respectively. (P) indicates where YM758 and/or its metabolites are transported via the passive diffusion process.

DMD Fast Forward. Published on March 10, 2008 as DOI: 10.1124/dmd.108.020669
This article has not been copyedited and formatted. The final version may differ from this version.

Table 1. Summary for K_m and IC_{50} values obtained in this study.

Cell lines	Substrate	Inhibitor	K_m (μmol/l)	IC_{50} (μmol/l)
mock-HEK293	YM758	-	135	-
rOct1-HEK293	MPP	YM758	-	23.8
rOct1-HEK293	metformin	YM758	-	<10.0
hOCT1-HEK293	MPP	YM758	-	40.5
OATP1B1-HEK293	$E_2$17βG	YM758	-	13.0
LLC-MDR1	YM758	-	20.9	-
human hepatocyte	YM758	-	87.9	-
human hepatocyte	YM758	quinidine	-	147

The concentration-dependent uptake and inhibition profile of YM758 were investigated using mock, rOct1, hOCT1 and OATP1B1-HEK293 cells, LLC-MDR1 cell, and human hepatocytes. The K_m and IC_{50} values were determined by nonlinear regression analysis as described under *Material and Methods*.

Fig.1

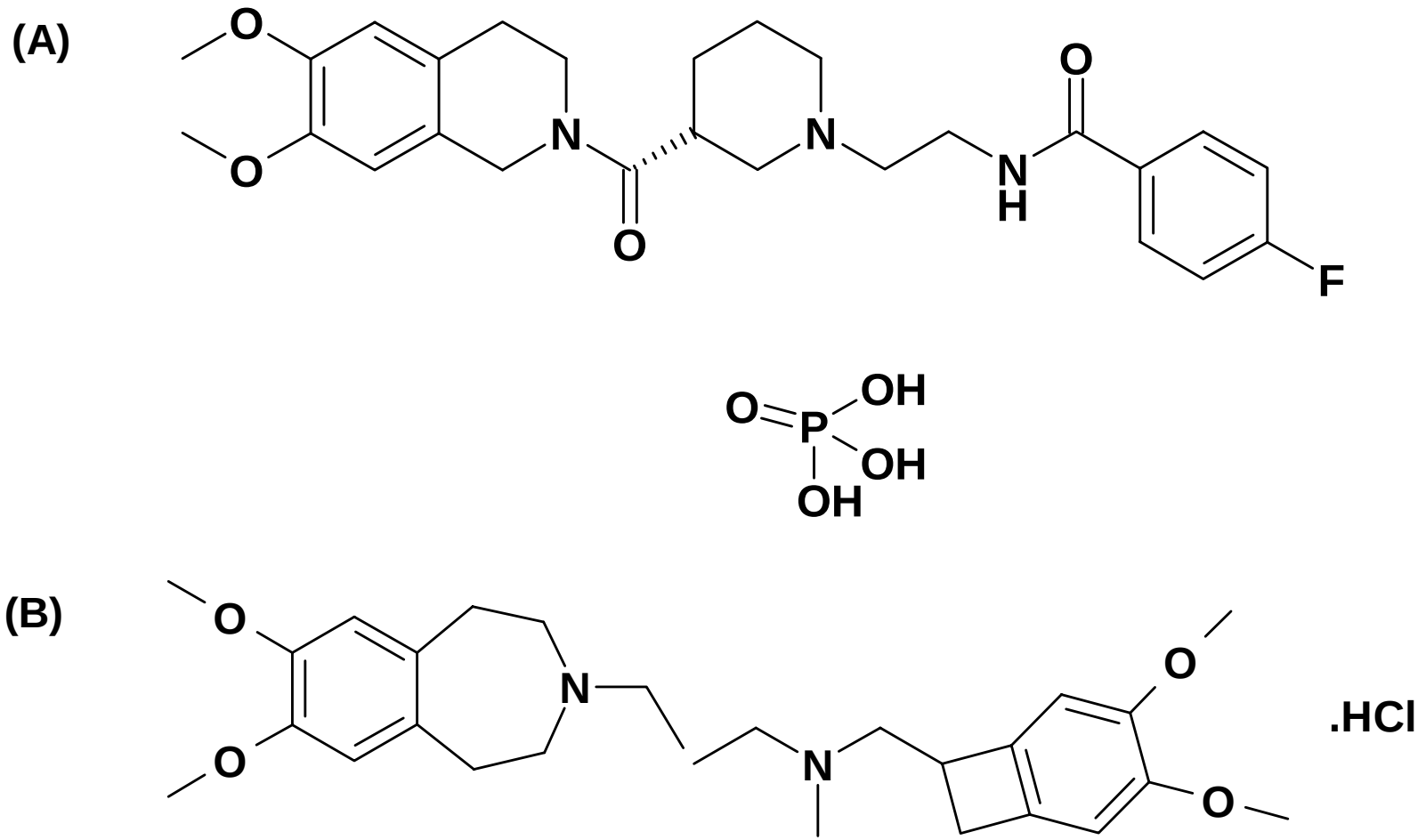

Fig.2

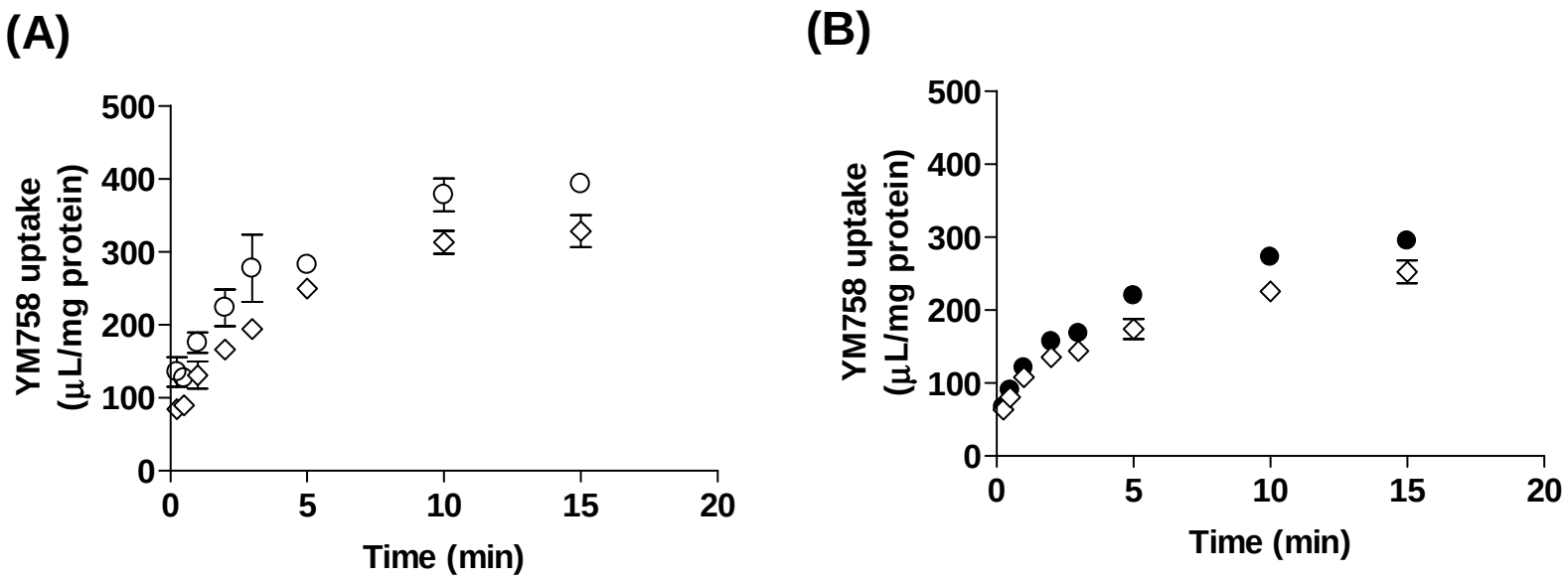

Fig.3

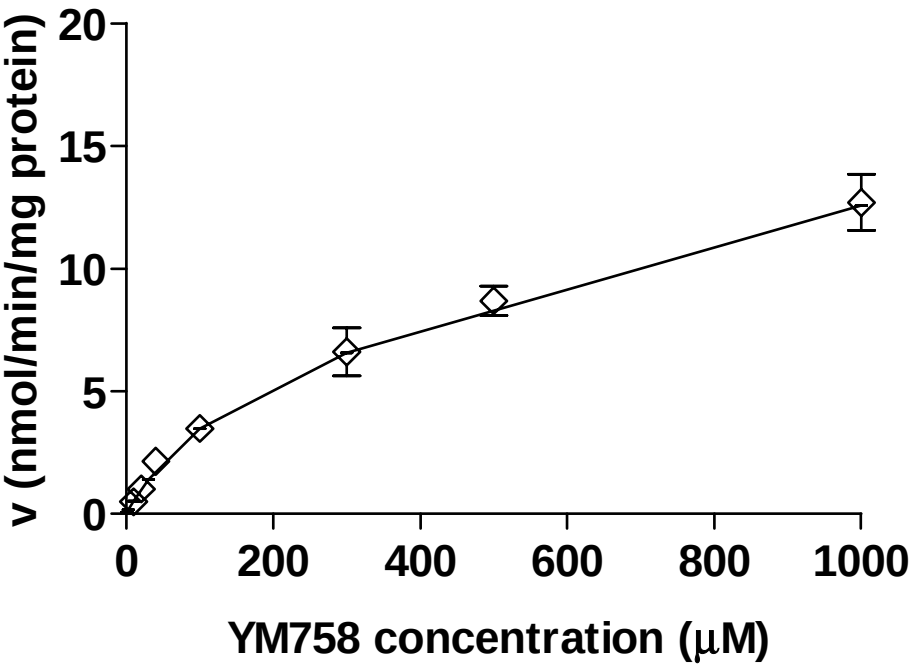

Fig.4

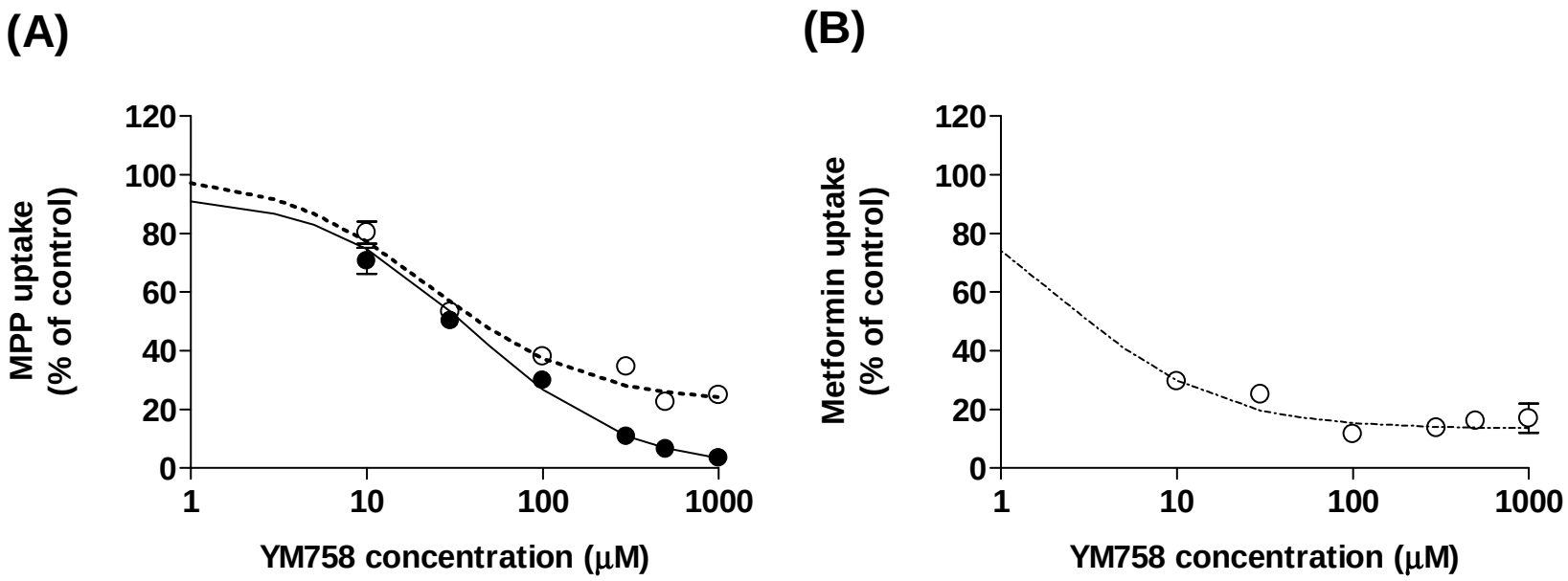

Fig.5

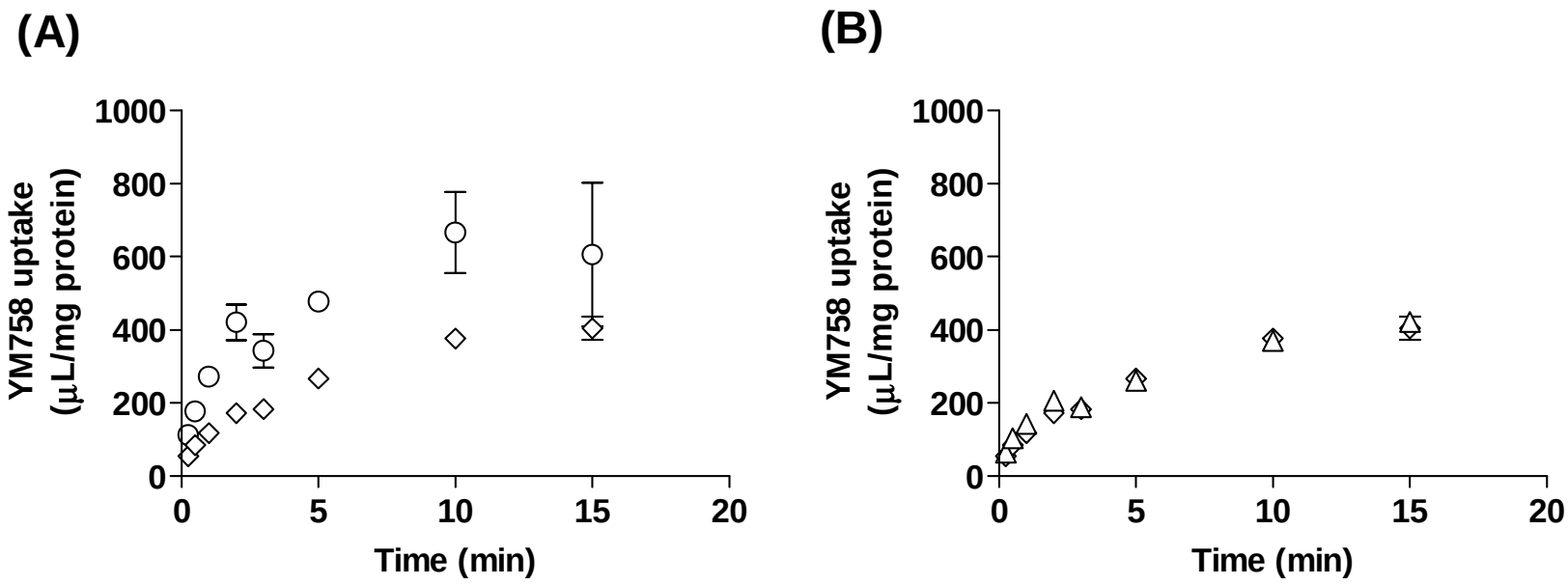

Fig.6

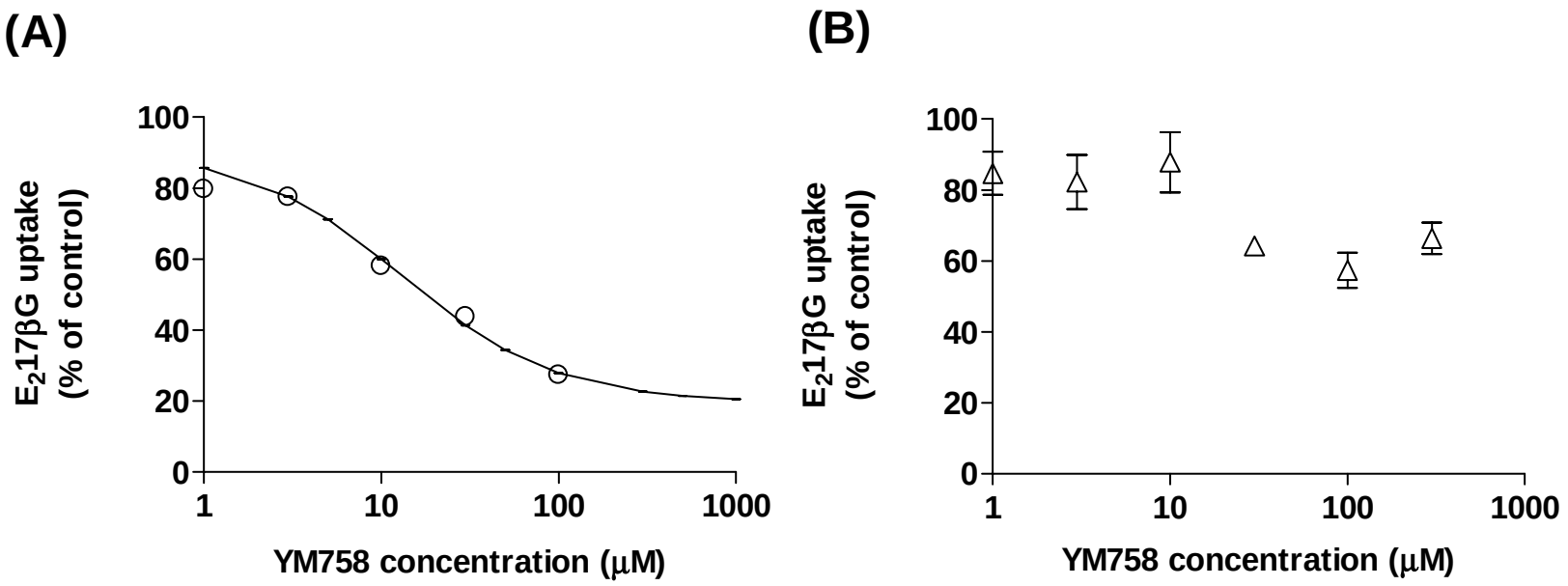

Fig.7

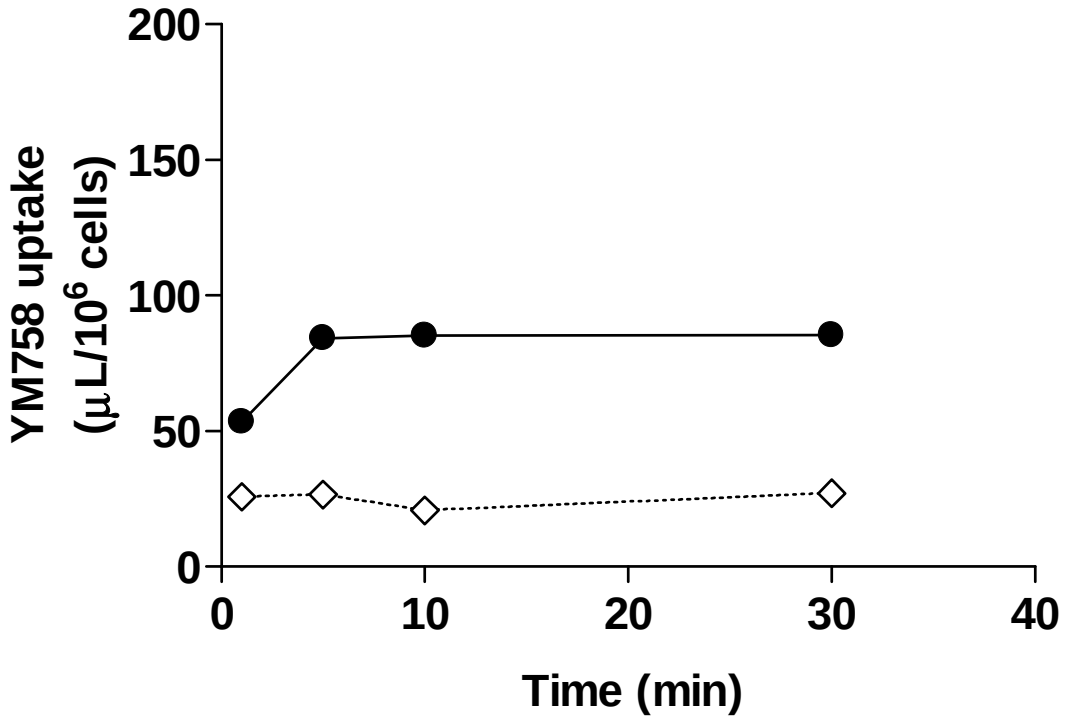

Fig.8

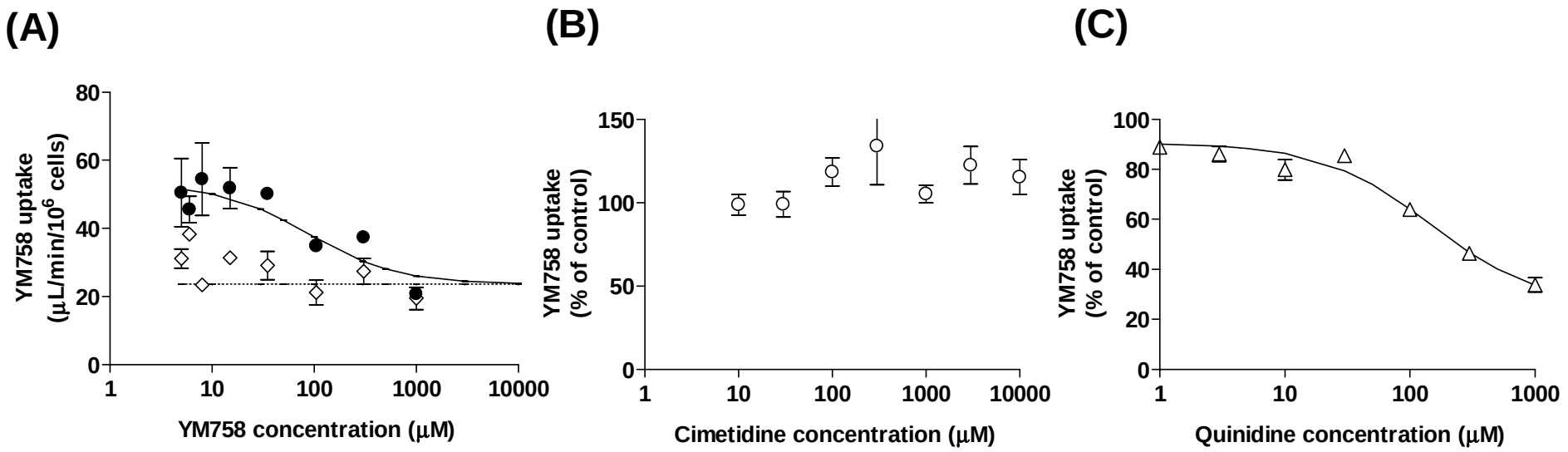

Fig.9

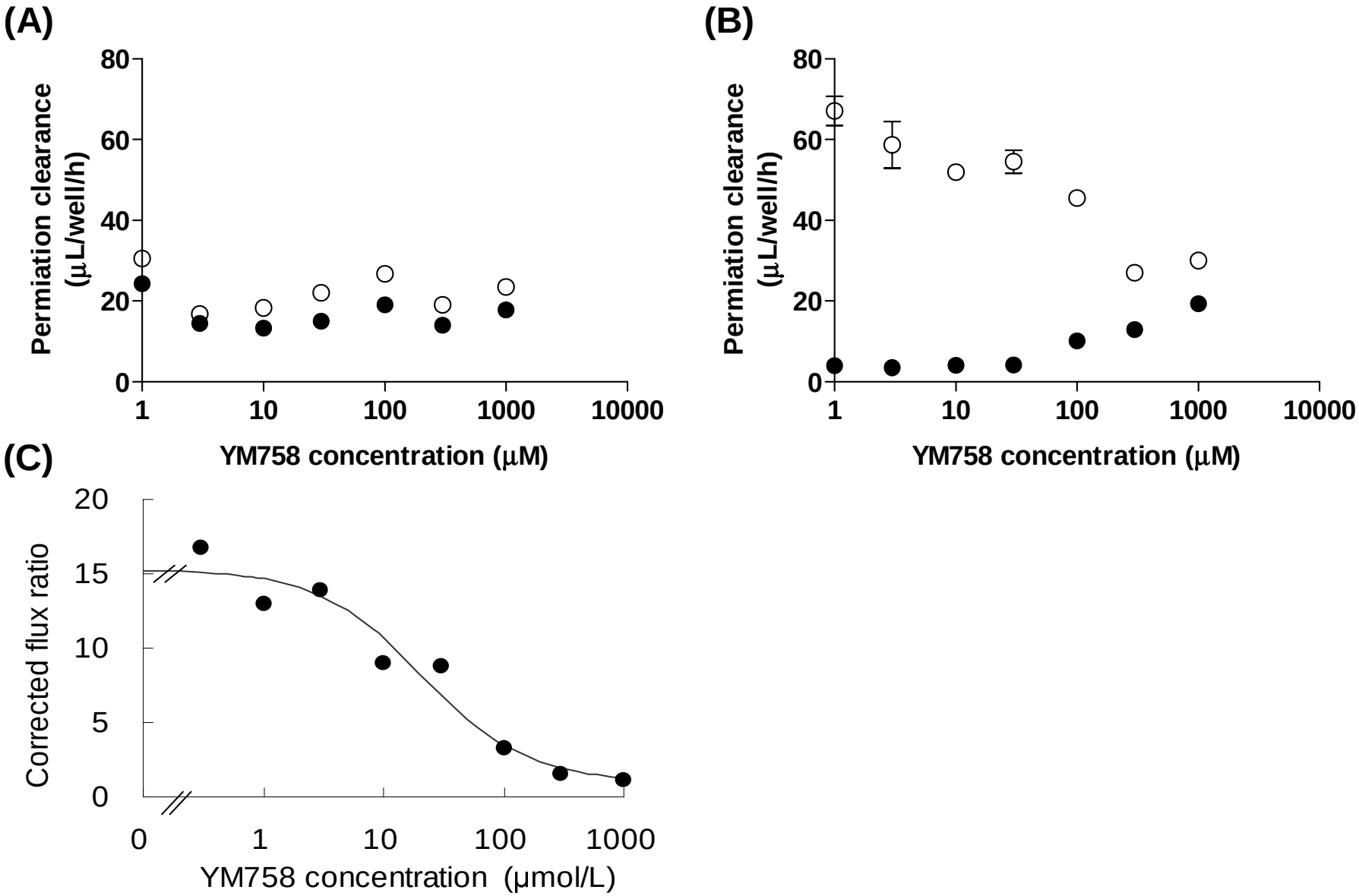

Fig.10